European Conference on Computational Fluid Dynamics
ECCOMAS CFD 2006
P. Wesseling, E. Oñate, J. Périaux (Eds)

SINGLE TRAIN PASSING THROUGH A TUNNEL

Jakub Novák*

*Skoda Research, Dep. of Fluid Mechanics,
Tylova 57, 316 00 Pilsen
Czech Republic
e-mail: jakub.novak@skoda.cz
Web page: http://www.skodavyzkum.cz

Key words: CFD, External Aerodynamics, Railway Application, Drag, Pressure Variations

Abstract. *The contribution deals with numerical solution of a complex problem of aerodynamic loads evoked by a train motion while entering and passing through a double track tunnel. The train set consists of an electrical loco and three coaches. The loco model shape closely corresponds with a real three-system electrical locomotive developed and produced by ŠKODA. The train performs a straight movement of 200 km/h speed rate. The main goal of the contribution is to monitor both the train motion aerodynamic effects on environment (tunnel wall surface) and backward effects of surrounding objects especially on loco body. Most of the results represent time variations of pressure, aerodynamic drag and velocities monitored both on tunnel and loco surfaces and in specified locations in the domain. Some of the values computed are compared with admissible limits published in adjacent standards*[3,4].

1 INTRODUCTION

ŠKODA TRANSPORTATION develops and produces a three-system electrical loco ŠKODA 109E, intended for train traction of EC/IC category and fast trains, as well as of fast goods-train on trackages of Czech Republic, Slovakia, Germany, Austria, Poland, Hungary and European Union corridors, electrified with systems 3 kVss, 25 kV/50 Hz and 15 kV/16,7 Hz (see Figure 1). As the loco surface design closely influences its external aerodynamic behavior when operating, there arise several problems suitable for numerical verification of correspondence with prescribed limits specified in standards[2,3,4]. The problem of a single train passing through a tunnel is specified in standard[3] in detail and a numerical solution of this problem presents this paper.

Aerodynamic loads represent an integral part of general loads that effect on operating rail vehicles. Highest values of rail vehicle aerodynamic loads can be reached along the entrance and passage through a tunnel. When a train passes through a tunnel, pressure waves are generated which propagate along the tunnel approximately at sonic speed. These pressure variations may pass into the interior of the trains, unless they are pressure sealed, and may cause discomfort to train passengers. The difference of pressure between outside and inside the vehicle will produce transient loads on the structure and on other vehicle components. Vehicle design shall be undertaken considering these effects.

Figure 1: The three-system electrical loco what’s model has been used for simulations

2 AERODYNAMICS IN TUNNELS – THEORY SHORTCUT

2.1 Aerodynamic resistance

As the drag may highly increase in a tunnel, it is also important to deal here with this additional source of resistance. In a tunnel, the same resistance to motion formula as in the open air can be used under otherwise identical conditions (straight and level track, constant speed), the only modification is the introduction of a tunnel factor T_f in the third term:

$$R = C_1 + C_2 v_{tr} + T_f C_3 v_{tr}^2 \quad , \tag{1}$$

where C_1 represents the rolling resistance, $C_2 v_{tr}$ the momentum resistance and $C_3 v_{tr}^2$ the aerodynamic drag. The tunnel factor T_f is the ratio (≥ 1) of the tunnel drag by the open-air drag. It varies during the train passage through the tunnel.

The increase of drag in a tunnel expressed by T_f depends on many factors; the blockage ratio B of the train in the tunnel is by far the most important of them:

$$B = \frac{S_{tr}}{S_{tu}} \quad , \tag{2}$$

where S_{tr} is the cross sectional area of the train and S_{tu} is the cross sectional area of the tunnel. But the type of the train and its length also have to be considered, as well as, at least for short tunnels (< 2000 m), the tunnel length and the train speed.

2.2 Pressure transients

When a train enters a tunnel, a compression wave is induced propagating along the tunnel with sonic speed (see Figure 2). This wave is reflected at the opposite portal as a rarefaction wave. When the rear of the train enters the tunnel, a rarefaction wave is produced again propagating along the tunnel relative to the moving air with sonic speed. This wave is reflected at the opposite tunnel end as a compression wave. These two waves are the main waves and they are always reflected at portals with opposite sense. Minor waves are caused by the passage of these waves over the train head and the train tail and so a very complex wave pattern is generated.

Depending on the location in the tunnel, the pressure histories can be very different. Further localized pressure changes are caused when the train head passes (pressure drop) and when the rear of the train passes (pressure increase).A typical pressure history at a point in the tunnel for a train passage is shown in c in Figure 1. The pressure distribution at a point on the train looks different (see b in Figure 2).

The intensity of the head entrance wave is a typical measure for the pressure history of a train passage. For aerodynamically well-shaped trains and small values of B the loss coefficient ζ_h (depending on the shape of the train head) can be neglected. For this case the pressure increase is function of the train speed v_{tr} and the blockage ratio B only:

$$\Delta p = p - p_0 \approx \frac{\rho v_{tr}^2}{2} \frac{2B}{1-2B} \tag{3}$$

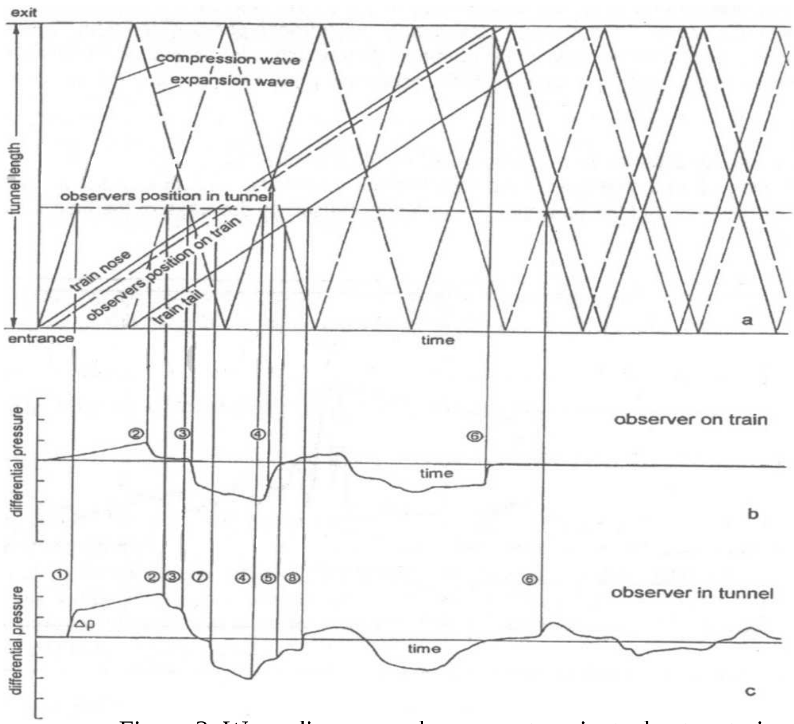

Key

1 Initial head wave
2 Initial tail wave
3 1st Reflection head wave
4 2nd Reflection head wave
5 1st Reflection tail wave
6 Exit wave
7 Passing of head
8 Passing of tail

Figure 2: Wave diagram and pressure transients due to a train passage through a tunnel

2.3 Flow velocities

The propagating pressure waves induce a flow in a tunnel. The headwave of the train causes a flow in the direction of train motion between the front of the wave and the train head. In the gap between the tunnel wall and the train wall there is a flow to the entrance portal during the entrance phase of the train. Due to the reflections of the pressure waves a very complex flow field in space, especially if the track is not in the center of the tunnel cross-section.

The induced flow velocity depends on the train speed v_{tr}, the blockage ratio B, the length of the train L_{tr}, and of the tunnel L_{tu} respectively, the roughness of the train and the tunnel wall respectively and on the initial air speed in the tunnel. The highest value of the flow speed is normally caused by the wake of the train after the main end has passed.

3 NUMERICAL SIMULATION

All the numerical simulations mentioned have been performed with professional software package Fluent, version 6.2, including the preprocessors Gambit and Tgrid.

3.1 Computational domain

General proportions of the 3D computational domain takes into account both volumetric needs of the problem (resulting from the tunnel and train proportions prescribed as well as from the sliding mesh method applied for the train movement simulation) and computational power available on the other hand, see Figure 3.

In Table 1 there are the main domain features' proportions compared with recommended values achieved from relations published in draft of standard[4] for testing and measurements. The clear difference should be noticed.

	Model (eq.)	**Standard[2,3] (eq.)**
Train set length [m]	84	-
Blockage ratio [-] (for double track tunnel)	0.15 (2)	0.18
Distance between the entrance portal and the monitoring point in tunnel [m]	50	202 (4)
Tunnel length [m]	100	832 (5)

Table 1 : Proportional characteristics of the domain in compare with recommendations from literature

In the Table 1, next relations have been used. The equation for the distance x_p between the entrance portal and the monitoring position is:

$$x_p = \frac{cL_{tr}}{c - v_{tr}} + x_1 \quad , \tag{4}$$

where L_{tr} is length of the train and the additional distance x_1 ensures a good separation of the individual waves and ideally should be about 100 m.

The equation for the minimum double track tunnel length is:

$$L_{tu,\min} = \frac{x_p}{2}\left(1+\frac{c}{v_{tr}}\right)+\Delta L_1 \quad , \tag{5}$$

where the additional length ΔL_1 ideally should be about 150 m.

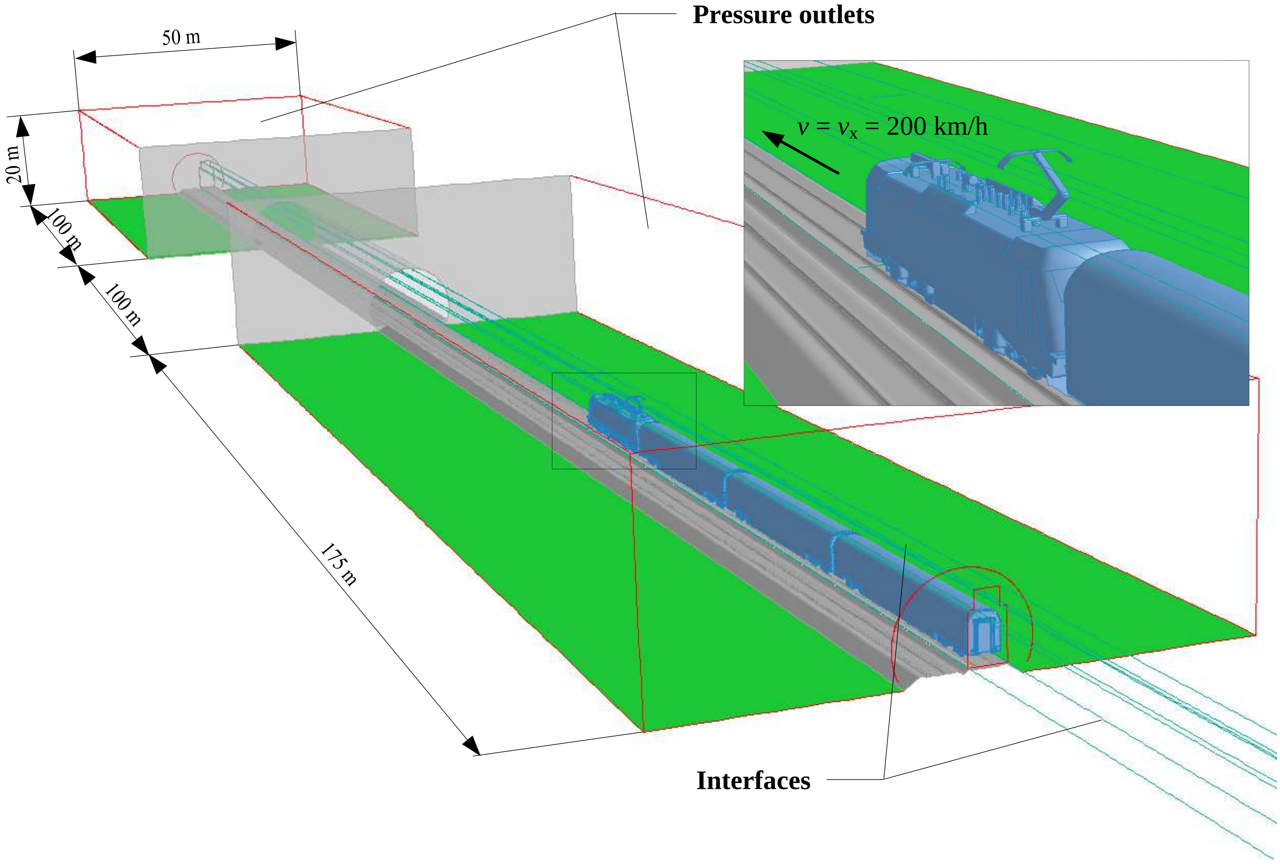

Figure 3: Computational domain at the starting position of the train (t = 0)

The domain features (rail, tunnel, train) correspond with proportions and shapes to real objects, see Figure 3. The tunnel portal is modelled as a vertical flat wall orthogonal to the train motion direction. This case represents the worst case that can occur.

To economize the problem, the whole domain has been further divided into several parts to enable meshing of particular volumes separately. So the closest neighborhood of the loco was meshed with relatively fine tetrahedral mesh, while on the rest of the domain coarser hexahedral mesh could be applied. Non-connected coincident interfaces of neighbouring parts of the domain with different face meshes were merged one to another into non-conformal grid interfaces prior to starting the calculation. General number of grid cells exceeded 2 million.

3.2 Sliding mesh model

When a time-accurate solution for two (and more) relatively moving object is desired, the only one possibility in Fluent to compute the unsteady flow field is usage of sliding mesh model. The sliding mesh model is the most accurate method for simulating flows in multiple moving reference frames, but it is also the most computationally demanding.

In sliding mesh technique two or more cell zones are used. Each sell zone is bounded at least one “interface zone” where it meets the opposing cell zone. The interface zones of adjacent cell zones are associated with one another to form a “grid interface”. The two zones move relative to each other along the grid interface (see Figure 3). Further information about the sliding mesh model can be found in literature[5].

3.3 Numerical solution and settings

Regarding to higher velocities expected (M > 0.25), the air flow was solved as an unsteady turbulent flow of compressible viscous Newtonian fluid with characteristics described in Table 2. The realizable k-ε turbulent model with the default values of model constants was used to compute turbulent kinetic energy and turbulent energy dissipation rate.

At the computational domain boundary following conditions have been set. On boundaries limiting the open spaces ahead and behind the tunnel, the pressure outlet boundary condition ($p_{st} = p_{atm} = 101325$ Pa) has been applied, while the ground, rail, tunnel and train set surfaces were defined as a solid wall. The speed of train motion, defined by the whole “tube” zone speed of motion, was set to 200 km per hour. As described in paragraph 3.2 above, the tube cell zone is separated from the rest by interface zone, defined on both the tube and the rest of the domain contacting surfaces. See Figure 3.

Characteristic	**Value**
Density [kg/m^3]	Ideal-gas law
c_p [J/kg-K]	1006.43
Thermal conductivity [W/m-K]	0.0242
Viscosity [kg/m-s]	$1.7894 \cdot 10^{-5}$
Molecular weight [kg/kmol]	28.966

Table 2 : Material characteristics of the air

For numerical computations, the segregated solver in 3D based on the unsteady implicit formulation of the second order upwind scheme has been used. Regarding to calculation stability, for pressure computing the default first order upwind scheme was conserved.

Fluent adaptive time stepping method was used for the time dependent solution. 20 iterations per time step appeared to be enough for proper convergence. See Table 3 for further details. Within the whole physical time, the residuals of all variables solved dropped below the 10^{-3} ratio in each time step, below the 10^{-7} ratio for energy equation respectively.

Parameter	Value
Truncation error tolerance	0.05
Ending time [s]	5.22
Minimum time step size [s]	0.008
Maximum time step size [s]	0.1
Minimum step change factor	0.5
Maximum step change factor	5
Number of fixed time steps	1

Table 3 : Adaptive time stepping method parameters

4 NUMERICAL RESULTS OUTLINE

According to the events mentioned in the theoretic sections above, the main part of computed results deals with time-variations of the loco aerodynamic drag, static pressure values on specified surface locations and *x*-component of velocity vectors in points positioned in the gap between the train wall and the tunnel wall. Other results introduce surface layout of pressure contours and velocity vectors. Some of the results obtained are compared to time progressions and marginal acceptable values published in adjacent standard[2].

4.1 Aerodynamic forces

Along the computation, there was monitored a time dependence of aerodynamic drag effecting on the loco in the opposite direction to train motion, see Figure 4. In fact, Figure 4 represents the time progression of the third term in equation (1), as indicated in section 2.1. The Figure also documents the refining influence of compressibility on numerical results.

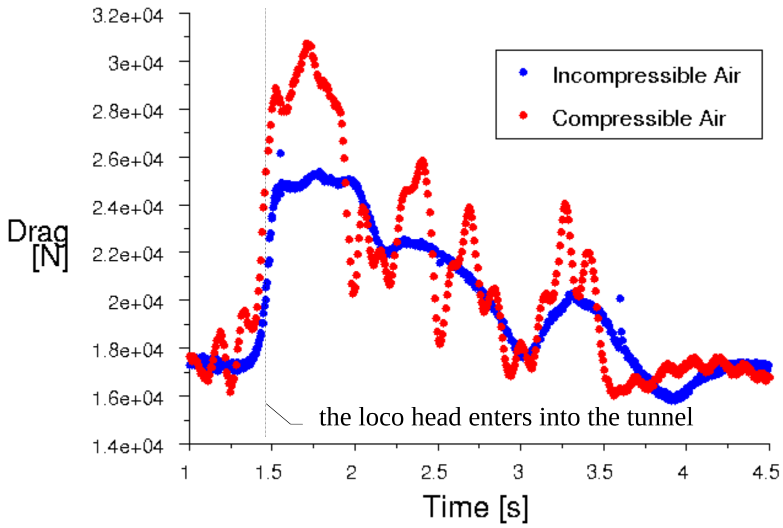

Figure 4: A time-progression of the loco aerodynamic drag within the tunnel passage

4.2 Pressure transient

In this section, time progressions of static pressure are monitored on wall surfaces as they are specified on the next figures. On Figure 5, there can be seen average values of static pressure on facets signed T1 – T3 over the whole train passage duration. The three facets positions are the clear from the upper picture.

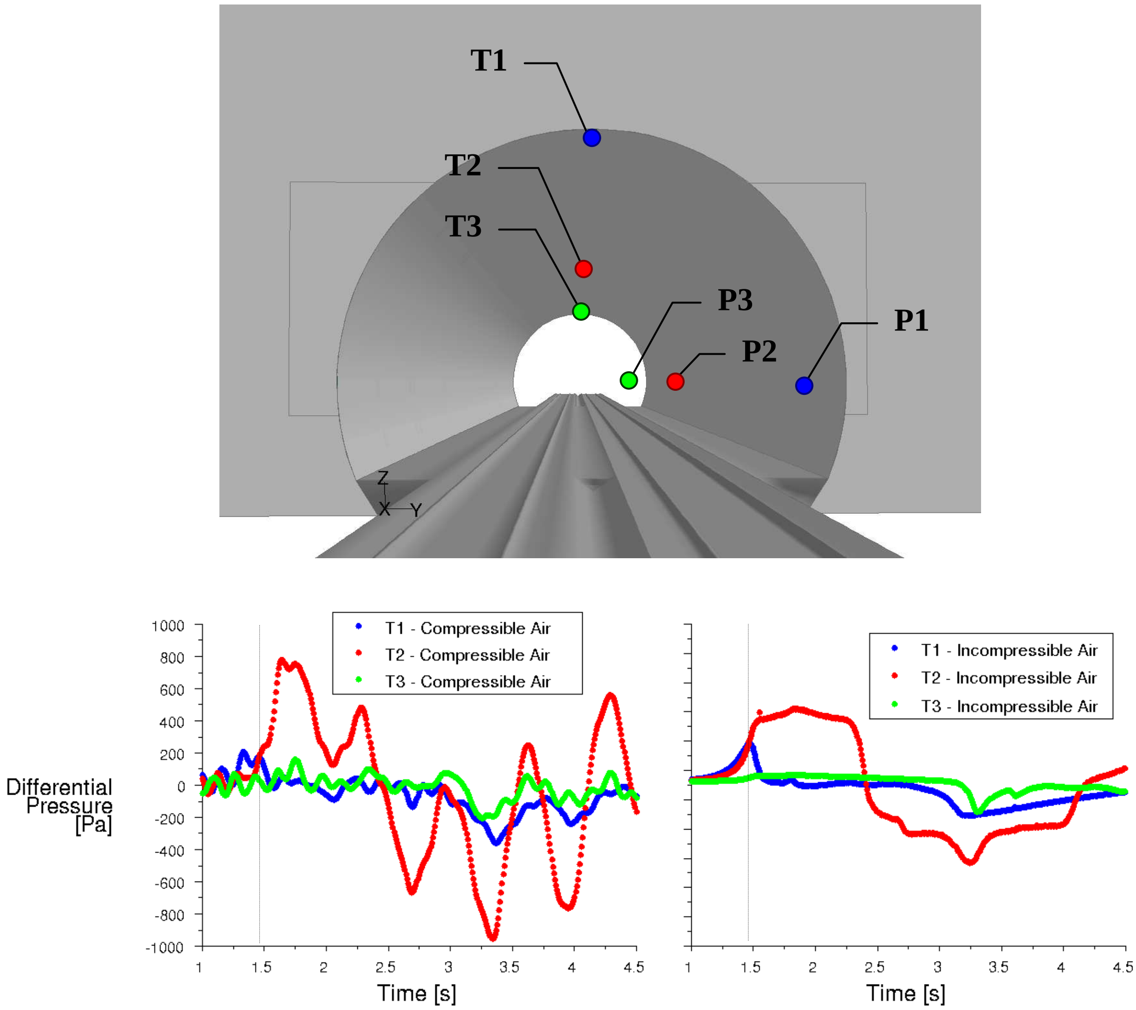

Figure 5: Facet average values of static pressure in monitoring facets on the tunnel wall surface over the whole train passage duration for compressible (left) and incompressible (right) air modeling

Similar to the tunnel surface, the progressions of static pressure can be monitored on the moving vehicle surface. On Figure 6 (upper), there is the locomotive model displayed with several loco surface sections highlighted (windows, doors, air-conditioning system inlets and outlets, or simply other segments of the loco surface). Only for some of them (with the titles L1 – L5) there are presented time variations of differential static pressure values, averaged over the surface area.

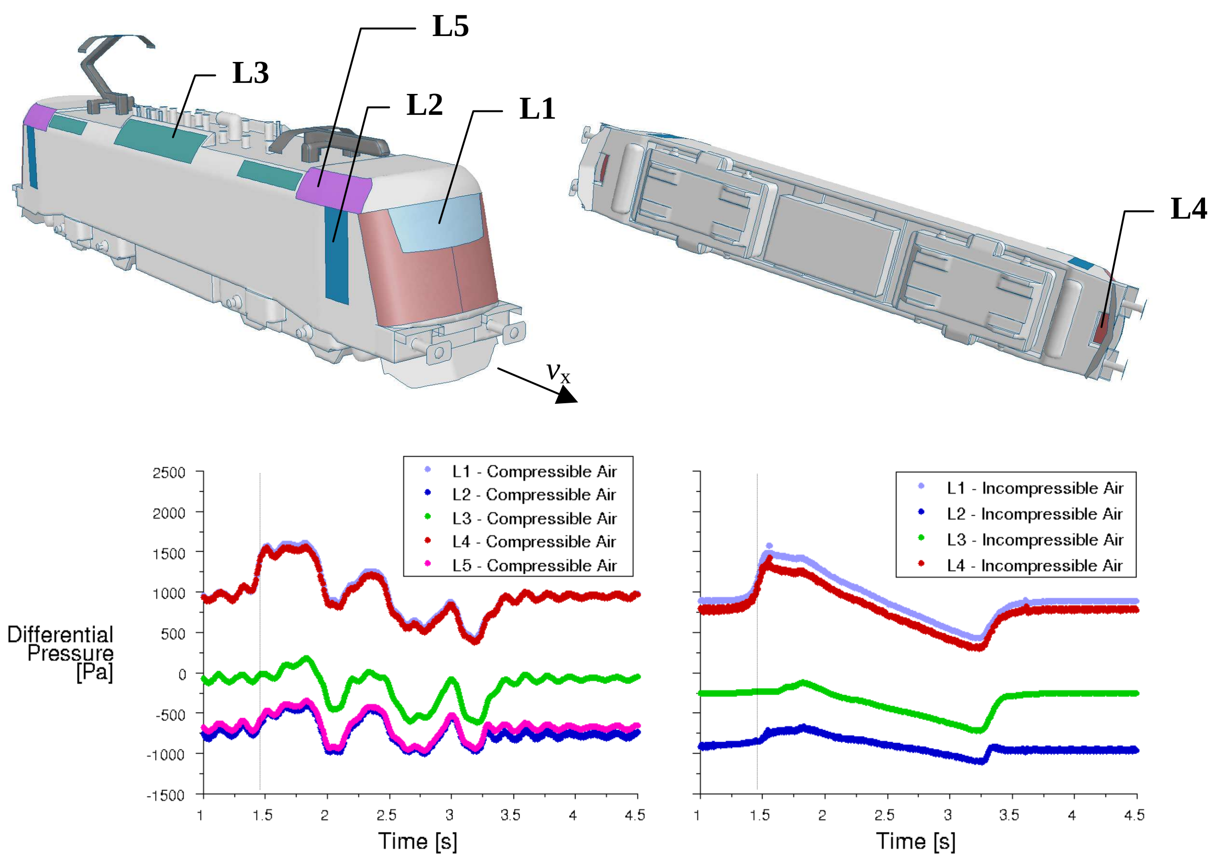

Figure 6: Facet average values of differential static pressure on selected monitoring facets of the locomotive surface over the whole train passage duration for compressible (left) and incompressible (right) air modeling

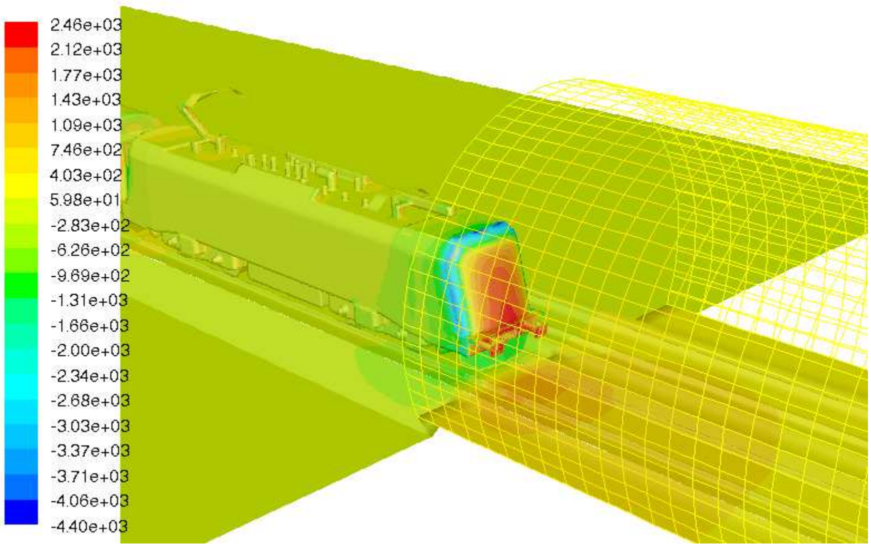

Figure 7: Surface differential static pressure on the locomotive head just entering the tunnel portal

Beside the graphical visualization, the relative effects between the train and the tunnel can be illustrated by surface isolines. On Figure 7, there is shown a layout of static pressure isolines on the locomotive surface at the position of the loco head just entering the tunnel portal (t = 1,44 s).

4.3 Air flow velocities

A layout of velocity vectors in a vertical intersection of the domain, at the moment when a loco head passes the entrance tunnel portal, is shown on Figure 8. In the gap between the tunnel wall and the train wall there is a flow in the opposite direction to the train motion clearly shown up.

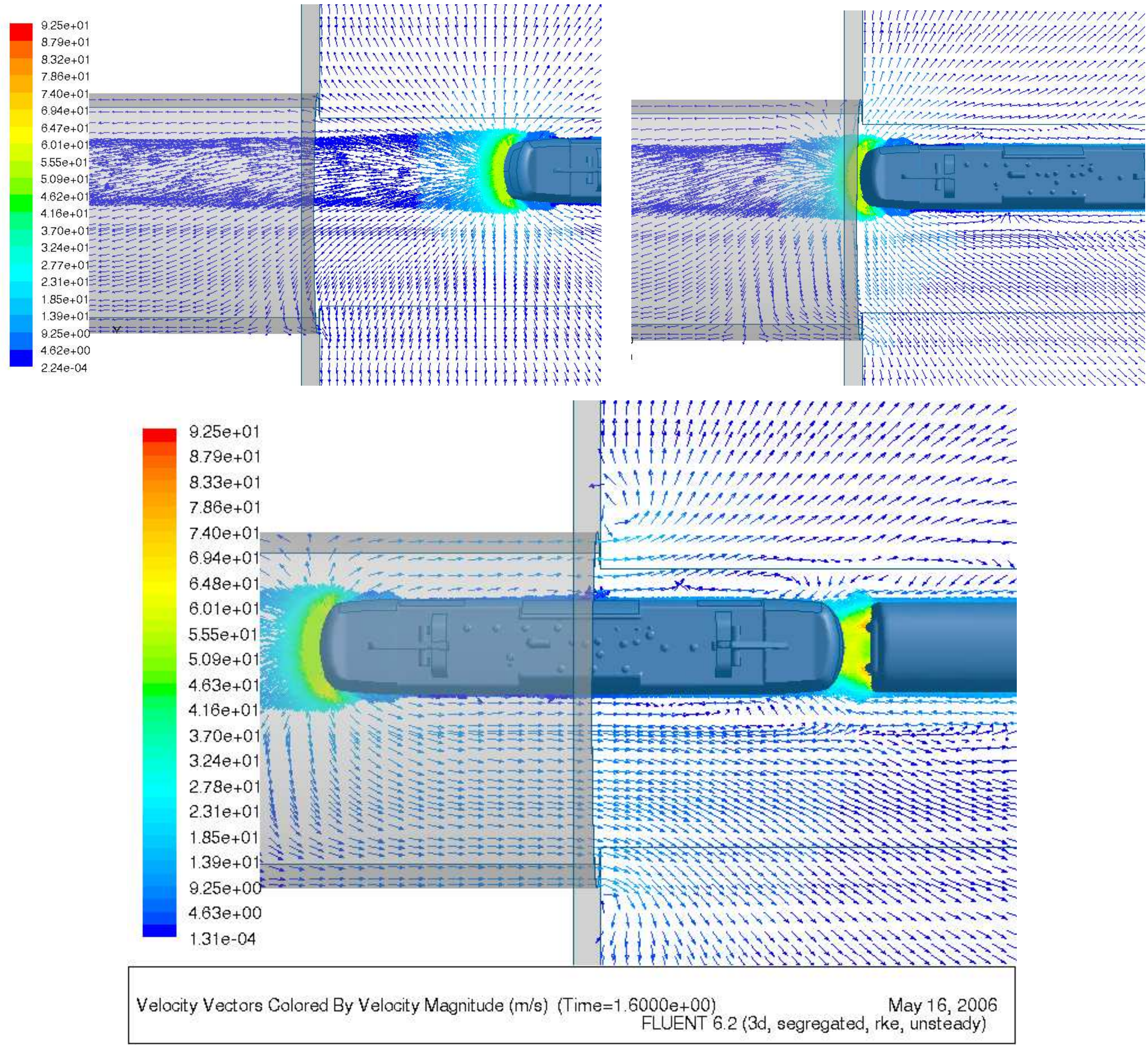

Figure 8: Velocity vectors in a vertical intersection of the domain for three different train positions when entering the tunnel

On Figure 9 there are displayed time behaviors of an *x*-component of velocity vector in points P1, P2 and P3 located on Figure 5. A rapid decline of the velocity, which propagates with the train movement, is caused by the headwave of the train.

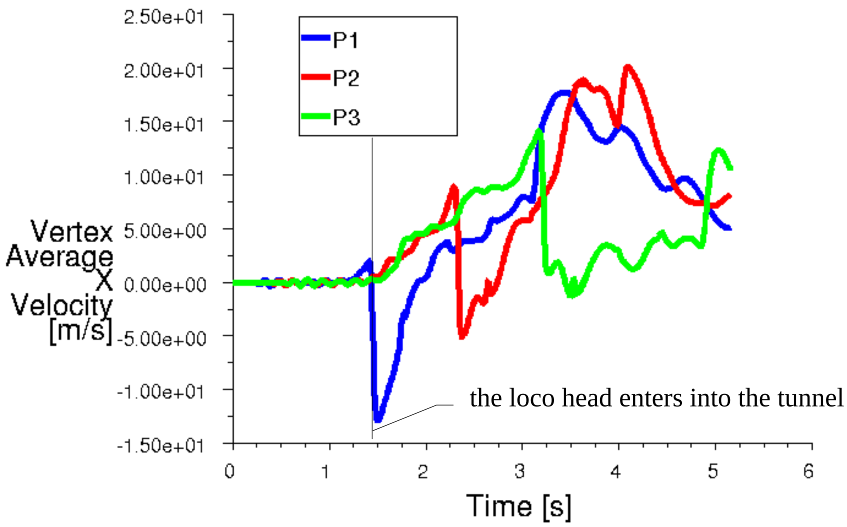

Figure 9: Time-progressions of *x*-velocity component monitored in three points P1 – P3 (see Figure 5 for positions)

5 CONCLUSIONS

Presented results of numerically solved aerodynamic problem of a single train passing through a tunnel approximately agrees with the presumptions given upon the relevant standards[3,4].

In a draft of standard[4] there is determined a medical health limit, that prescribes the maximum pressure change (peak-to peak) to which train passengers and crew are subjected. It shall not exceed 10 kPa within any part of the time taken by the train to pass through any particular tunnel and operational situation. When looking back, any of the pressure changes presented within this contribution do not reach this value by far. There can be several reasons, why this is:

- The maximum (modeled) train speed of motion is not so high to induce such pressure deviations.
- The tunnel length modeled is not sufficient, increasing length of the tunnel will cause higher pressure changes.
- The value of aerodynamic pressure variations considered occur only in extremely rare emergency conditions – normal rail operations will not involve conditions of this severity.
- The surface design of the three – system locomotive SKODA is well shaped.

As to the problem solved, further effort will be aimed to eliminate “secondary pulsations” (especially of pressure), which occurred when the solution for compressible air flow is realized. The possibilities to improve the solution seem to be in the computational grid quality eventually in numerical solution controls.

In connection with numeric solutions realized, there is an exertion spent on preparation and realization of operation tests on proving track to validate the obtained numeric results expertly. Participation in the project of the Research Centre of Rail Vehicles supported by the Czech Ministry of Education, Youth and Sports gives a real outline, how to reach it.

Acknowledgements

This contribution includes partial results from the project 1M0519 – Research Centre of Rail Vehicles supported by the Czech Ministry of Education, Youth and Sports to which we express our grateful thanks.

REFERENCES

[1] European Standard EN 14067-1, "*Railway application – Aerodynamics – Part1: Symbols and units*", Comité Européen de Normalisation (CEN), Brussels, (2003).
[2] European Standard EN 14067-2, "*Railway application – Aerodynamics – Part2: Aerodynamics on open track*", Comité Européen de Normalisation (CEN), Brussels, (2003).
[3] European Standard EN 14067-3, "*Railway application – Aerodynamics – Part3: Aerodynamics in tunnels*", Comité Européen de Normalisation (CEN), Brussels, (2003).
[4] European Standard Draft prEN 14067-5, "*Railway application – Aerodynamics – Part5: Requirements and test procedures for aerodynamics in tunnels*", Comité Européen de Normalisation, Brussels (CEN), (2003).
[5] Fluent Inc., *Fluent 6 User's Guide*, Vol. II, (2001)
[6] J. Novák, "Study of Aerodynamical interaction between 109E locomotive and wagon with CFD use", *Proceedings of the 3rd International Conference on Dynamics of Civil Engineering and Transport Structures and Wind Engineering*, 20-23 (2005), (in Czech).